Colloid Polym Sci (2002) 280: 607–615
DOI 10.1007/s00396-002-0667-2

ORIGINAL CONTRIBUTION

Minseok Seo
Eugenia Kumacheva

Response of adsorbed layers of hydroxypropyl cellulose to variations in ambient humidity

Received: 25 May 2001
Accepted: 16 January 2002
Published online: 8 May 2002

M. Seo · E. Kumacheva (✉)
Department of Chemistry,
University of Toronto,
80 St. George Street, Toronto,
Ontario M5S 3H6, Canada
E-mail:
ekumache@alchemy.chem.utoronto.ca

Abstract The surface force balance technique and atomic force microscopy were used to study variations in the properties of adsorbed hydroxypropyl cellulose (HPC) layers as a function of ambient humidity. The relative humidity was varied from 0 to 97%. It was found that the fiberlike HPC layers shrink following adsorption of moisture. On the basis of the observed variation in the thickness and compressibility of the HPC layers, the hysteresis noted in its compression–decompression cycles, and the recovery of the properties of the layer upon drying, we proposed a two-step mechanism of water sorption by fibers of HPC. In the first stage, adsorption of moisture is dominated by capillary condensation in the voids and capillaries of the fiberlike HPC layer. In the second step, water penetrates inside the fibers and forms a surface gel, whereas the inner cores of the fibers retain their rigidity.

Keywords Surface forces · Atomic force microscopy · Hydroxypropyl cellulose · Relative humidity

Introduction

Cellulose derivatives are used as viscosity modifiers in waterborne paints [1], steric stabilizers of colloid particles [2], advanced humidity sensors [3], binders in the granulation of pharmaceutical powders, and materials for drug encapsulation [4, 5] and papermaking [6]. Owing to the limited flexibility of their molecules, cellulose polymers form lyotropic liquid-crystalline phases [7]; this feature has potential applications in the development of materials for nonlinear optics.

In all these applications, the performance of cellulose polymers depends critically on their interactions with water. For example, when cellulose derivatives are used for vaccine and drug encapsulation, penetration of moisture through the polymeric shell influences the properties of drugs during storage. On the other hand, in vivo swelling and dissolution of polymeric shells control the speed of drug release and the transportation of the drug to the required location. In another application, when cellulose polymers are used as humidity sensors, the efficiency of the sensor is determined by the speed and the magnitude of the material's response to small variations in ambient humidity, as well as by the reversibility of this response under conditions of increasing or decreasing humidity.

In many applications, cellulose polymers are used as thin, dry films, and the variations in their properties occur on a submicrometer level. Examination of the relationship between the amount of adsorbed moisture, the structure of the polymer layer, and the variation in the properties of the layer has stimulated substantial interest in recent years [3, 8, 9]; however, most of studies have focused either on characterizing the structure and composition of the cellulose films [8], or on the kinetics of water sorption [3, 9], or on changes in the mechanical properties of the cellulose films, such as puncture strength and elongation [10]. To the best of our knowledge, the relationship between these factors for thin, dry layers of cellulose derivatives has not been addressed.

Here, we employed the surface forces balance technique [11] and atomic force microscopy (AFM) to study

the effect of variations in ambient humidity on the properties of thin layers of hydroxypropyl cellulose (HPC) self-assembled from aqueous solutions on a mica surface. The variations in the thickness and the compressibility of the HPC layers were studied by examining the change in quasi-equilibrium normal interactions between the films following their exposure to water vapor. The ambient relative humidity (RH) varied in a stepwise manner from 0 to 97%. The results of studies of time-dependent shear interactions between HPC layers equilibrated under different RH conditions are reported elsewhere [12].

Experimental

Materials

HPC ($M_w = 370{,}000$), ethanol (spectrophotometric grade), and *n*-heptane (reagent grade) were purchased from Aldrich Canada. The water was distilled and passed through a Millipore Simplicity system. First-grade muscovite mica was purchased from S&J Trading (USA).

Prior to self-assembly of HPC on mica, the polymer was fractionated by the addition of *n*-heptane (nonsolvent) to a solution of HPC in ethanol (good solvent) [13]. Ethanol was distilled after refluxing it with magnesium metal strips, whereas *n*-heptane was dried by storing it for several days with sodium strips. About 8 g HPC was stirred at room temperature for 16 ± 2 h with a mixture of ethanol and *n*-heptane. The volume fraction of ethanol in the mixture varied from 0.35 to 0.45. The clear solution containing a lower-molecular-weight fraction of HPC was concentrated in a vacuum evaporator for 3 h at 35 °C. The undissolved gel was separated from the solution by decantation or centrifugation, dried, and then dissolved again in the solvent mixture richer in ethanol. After the completion of each step of the fractionation, the translucent HPC gel was separated from the supernatant liquid and the next step of the extraction was carried out. In this work, we used the polymer fraction with $M_w = 39{,}000$ and $M_n = 23{,}000$ determined by gel permeation chromatography.

Methods

Atomic force microscopy

Dry layers of HPC were imaged in contact mode with a Picoscan AFM (Molecular Imaging, Phoenix, Ariz.), using pyramidal silicon nitride tips. The cantilever spring constant was 0.58 or 0.38 N/m. Both height and deflection mode images were taken simultaneously. The scan rates varied in the range 1–2 Hz.

Freshly cleaved mica sheets were exposed to 10^{-3} g/ml aqueous solutions of HPC for 12 ± 1 h, after which they were washed in pure water, dried in a laminar flow cabinet for about 4 h, and then immediately examined by AFM. To image the structure of the HPC layer in water, a magnetic alternating current mode was employed, in which an oscillating magnetic field was used to drive the cantilever of the atomic force microscope with a spring constant of 0.1 N/m. The images presented in this work were obtained repeatedly in at least five different spots of the sample.

Surface forces measurements

The surface forces experiments were carried out using the surface forces balance technique described in detail elsewhere [11, 14]. The normal force, F, acting between the two macroscopic, atomically smooth mica plates was measured as a function of the distance, D, between the surfaces and the ambient RH. The measurements of D were carried out using the optical interference technique by monitoring the variations in positions of fringes of equal chromatic order (FECO). The results of the measurements are presented as force–distance profiles $F(D)/R = f(D)$, where R is the radius of curvature of the surfaces.

Back-silvered mica sheets with a thickness of about 2 μm were glued, using thermosetting epoxy glue EPON-1004, onto two cylindrical quartz lenses and mounted in a cross-cylindrical configuration into the surface forces apparatus (SFA). A beaker with P_2O_5 was introduced into the apparatus, and filtered dry nitrogen was purged through the chamber for 12 h. Then, the mica surfaces were brought in contact, and the "contact" position of the FECO was measured for $D = 0$. The apparatus was then brought into the laminar flow cabinet, and the lenses with the mica sheets were removed from the apparatus and immersed into the 10^{-3} g/ml solution of HPC for 12 h. Following the adsorption of HPC on the mica, the surfaces were washed with pure water, dried for about 4 h, and placed back in the instrument. A beaker with fresh P_2O_5 was introduced into the SFA, and the chamber was purged again with dry nitrogen for 12 h, after which the normal forces were measured between the mica sheets covered with the dry HPC layers. The surfaces were then separated to a distance of about 2–3 mm, and the RH in the surface force was increased in a stepwise manner by introducing into the SFA beakers with saturated salt solutions. The salt solutions used to control the vapor pressure in the apparatus and the corresponding values of the RH are shown in Table 1. The replacement of beakers containing salt solutions was carried out in the laminar flow cabinet in dust-free conditions. For each value of the RH, prior to measuring the surface forces, the HPC layers were equilibrated for about 24 h. For RH = 23%, the first measurement was done after 3 h. After finishing a series of experiments for increasing RH, the salt solutions in the SFA were subsequently replaced to decrease the humidity from 97 to 0%.

The SFA experiments were performed at 24 ± 1 °C. We report the results of four independent experiments.

Water sorption

Glass vials containing about 0.1 g HPC each were introduced into the sealed chamber. The value of the RH in the chamber was controlled either by introducing P_2O_5 and purging dry N_2 through it to achieve RH = 0 or by introducing into the chamber the saturated salt solutions listed in Table 1. For each value of the RH the system was equilibrated for 24 h, after which the vials with the HPC samples were weighed with an accuracy of 0.0002 g. To account for adsorption of water vapor by the glass walls of the vials, a control experiment was carried out for each value of the RH by measuring the change in the weight of an empty vial placed into the same chamber. For each value of the RH, two independent measurements were performed. The error in these experiments did not exceed $\pm 0.04\%$.

Table 1. Selected saturated salt solutions and corresponding values of relative humidity at 25 °C [26]

Electrolyte solutions	Relative humidity (%)
Potassium acetate	22.51 ± 0.32
Potassium carbonate	43.16 ± 0.39
Sodium chloride	75.29 ± 0.12
Potassium sulfate	97.30 ± 0.45

Results

The variation in the weight of HPC following adsorption and desorption of moisture at different ambient RH is shown in Fig. 1. In this graph, the concentration of water, ϵ, in the HPC sample is plotted as a function of RH, where $\epsilon = w_{RH} - w_{RH=0}/w_{RH}$; w_{RH} is the weight of the HPC sample after its equilibration for 24 h at a particular value of the RH and $w_{RH=0}$ is the weight of the sample in dry nitrogen. When the humidity increased, the amount of adsorbed moisture in the HPC gradually increased (Fig. 1, curve a). The sorption of water increased significantly for RH > 43%, and for RH = 97%, ϵ reached its maximum value of 18 wt%. In the next series of experiments, the RH in the chamber was reduced in a stepwise manner, and the decrease in the weight of the HPC was measured by following the water desorption (Fig. 1, curve b). The shape of the curve $\epsilon = f(\mathrm{RH})$ was similar to that obtained in experiments for increasing humidity; however, the process of water desorption occurred at a slightly slower speed, and for the same exposure time a larger amount of water was immobilized by the HPC layer. The difference in ϵ increased with the RH and for RH = 75% it was about 3 wt%.

Following these experiments, the structure of the self-assembled HPC layers was studied using AFM. The AFM images of the HPC layers adsorbed from polymer aqueous solution at $c_{HPC} = 1.0\times10^{-3}$ g/ml are shown in Fig. 2. Figure 2a shows the surface of the mica after 10-min exposure to the solution of HPC. Small globules of HPC with a diameter of about 40 ± 10 nm randomly covered the surface of the mica. Following a longer adsorption time of about 30 min, these globules developed into short rodlike structures with a thickness of about 40 nm and a length of about 150 nm, as shown in Fig. 2b. After 24-h adsorption, the HPC layer gained a well-defined, close-packed, fiberlike morphology (Fig. 2c). The individual fibers had a thickness about 170 ± 10 nm, and the root-mean-square roughness of the layer did not exceed about 5 nm. The adsorbed HPC layer was relatively soft, especially after exposure to water vapor, and repeated scans noticeably enhanced the orientation of the HPC fibers. Exposure of the HPC layers to water vapor did not change the layer

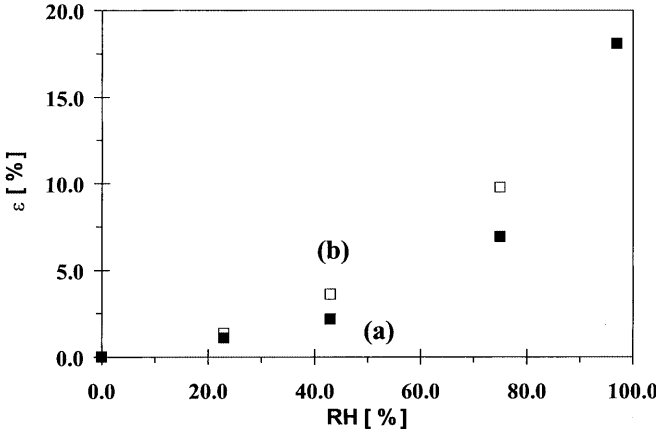

Fig. 1. Variation in the concentration of water, ϵ, in hydroxypropyl cellulose (*HPC*) as a function of relative humidity (*RH*). The *open* and the *filled symbols* correspond to experiments with increasing and decreasing humidity, respectively

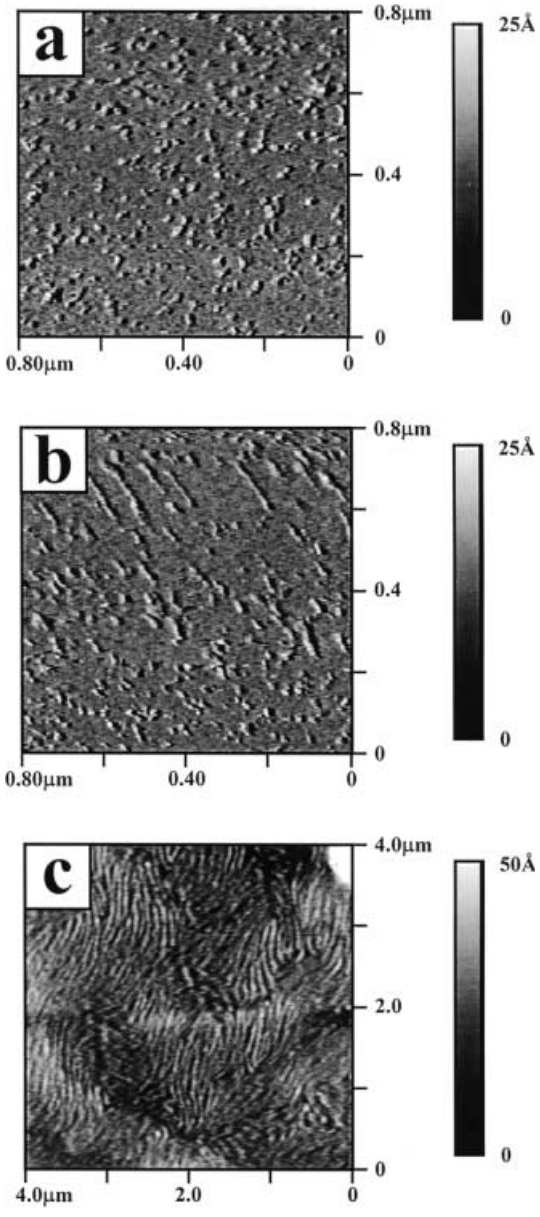

Fig. 2a–c. Atomic force microscopy images of the HPC layers adsorbed from 1.0×10^{-3} g/ml aqueous solution. Adsorption of HPC globules onto the mica surface after **a** 10 min, **b** 30 min, and **c** 12 h. **a** and **b** were taken in HPC solution. **c** was taken for RH = 0

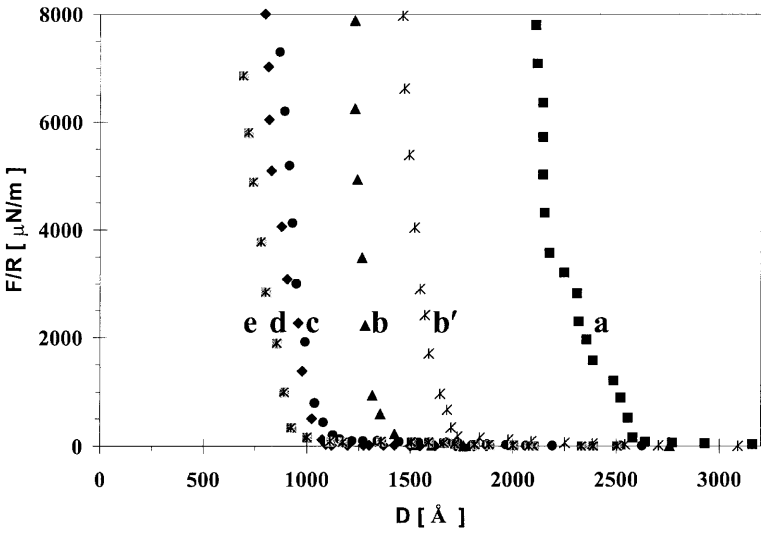

Fig. 3. Surface forces profiles measured on approach of HPC-covered mica surfaces equilibrated for 24 h under conditions of different ambient humidity: RH = 0% (*squares*); 23% (*triangles*), 43% (*circles*), 75% (*diamonds*), and 97% (*crossed squares*). Surface forces profile measured after 3 h exposure at RH = 23% (*stars*)

morphology, and even after equilibration at RH = 97% the layer retained its fiberlike structure.

The relatively minor roughness of the fiberlike HPC layers enabled us to examine these layers using the surface forces balance technique. Typical force profiles obtained by approaching the mica surfaces covered with HPC and measuring the normal quasi-equilibrium forces acting between them are shown in Fig. 3. For RH = 0 (Fig. 3, curve a) the onset of the long-range repulsion forces occurred at 2,750 ± 50 Å, while for $D < 2{,}300$ Å a "hard-wall" repulsion was measured and the surface separation did not decrease further for F/R exceeding 10^4 μN/m.[1] After increasing the RH to 23% and equilibrating the surfaces under these conditions for 24 h, the onset of repulsion shifted to about 1,500 Å (Fig. 3, curve b). The shift occurred relatively rapidly: when the surfaces were maintained at RH = 23% for 3 h, the force profile moved inwards 1,050 Å (Fig. 3, profile b′), while after another 21 h the onset of repulsion was changed by only 200 Å. A further shift in the onset of the repulsive forces to about 1,250, 1,100, and 1,050 Å was measured when the RH increased to 43, 75, and 97%, respectively (Fig. 3, profiles c–e), however, the decrease was less dramatic than that observed upon the increase of the RH from 0 to 23%. During compression, the force profiles measured for RH > 43% featured a relatively shallow initial increase in the repulsion force, which depended on the value of the RH. In contrast, the slope of the hard-wall part of the force–distance profiles showed a weak dependence on the RH.

Following measurements at RH = 97%, the humidity of the air in the SFA was reduced in a stepwise manner and the HPC layer "recovery" was studied by equilibrating the layer for about 24 h for each value of the RH. The recoveries of the position of the hard wall and the onset of normal interactions were determined separately, as is shown in Fig. 4. The former parameter was defined as $D_{HW,\ DH}/D_{HW,IH}$, where $D_{HW,DH}$ and $D_{HW,IH}$ are the distances between the mica surfaces for which hard-wall forces were measured in experiments with decreasing and increasing RH, respectively. The recovery in the onset of the surface interactions was characterized as $D_{0,DH}/D_{0,IH}$, where $D_{0,DH}$ and $D_{0,IH}$ are the separations between the surfaces at which repulsion between them commenced for decreasing and increasing RH, respectively (see inset to Fig. 4). A comparison of the $D_{0,DH}/D_{0,IH}$ ratios for different values of the RH shows that upon drying, the HPC layer completely recovered its original thickness; however, the position of the hard-wall part varied significantly for different RHs. For the high values of the RH (e.g. for 75%) almost complete recovery occurred ($D_{HW,DH}/D_{HW,IH} \approx 1$), while for the low values of the RH (0 and 23%) the position of the hard wall shifted inwards ($D_{HW,DH}/D_{HW,IH} < 1$), indicating that the layer was more compliant upon drying.

The effect of the RH on the response of the HPC layer in compression–decompression cycles was studied by comparing the force profiles measured on approach and separation of the surfaces. For RH = 97%, several contact times were examined, varying from about 2 to 20 min. The results of force measurements are presented in Fig. 5. The hysteresis in the surface force profiles measured on approach and separation of the HPC-covered surfaces depended on the value of the RH in the experimental chamber. For RH = 0%, the normal forces measured in compression–decompression cycles were somewhat different in the shallow part of the profile, i.e., repulsion commenced at a distance about 200 Å shorter upon their separation. However, in their rigid part the force profiles measured in compression and decompression were very close. No attraction was observed at

[1] The onset of repulsion was verified in several experiments and for several contact positions

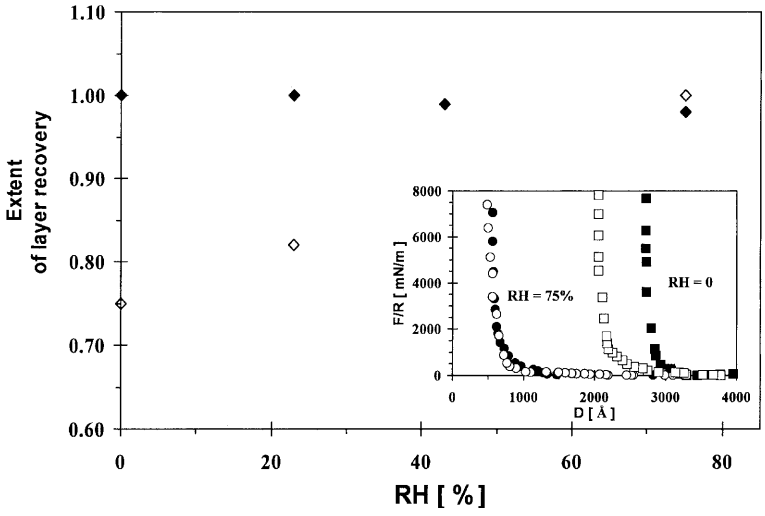

Fig. 4. Recovery of the adsorbed HPC layer based on comparison of force profiles shown in the *inset*. The recovery of the layer thickness (*filled diamonds*) was calculated as $D_{0,DH}/D_{0,IH}$ (see text). The recovery in the layer compressibility (*open diamonds*) was characterized as $D_{HW,DH}/D_{HW,IH}$. *Inset*: force profile measured following an increase (*filled symbols*) and a decrease (*open symbols*) in RH: 0% (*squares*) and 75% (*circles*)

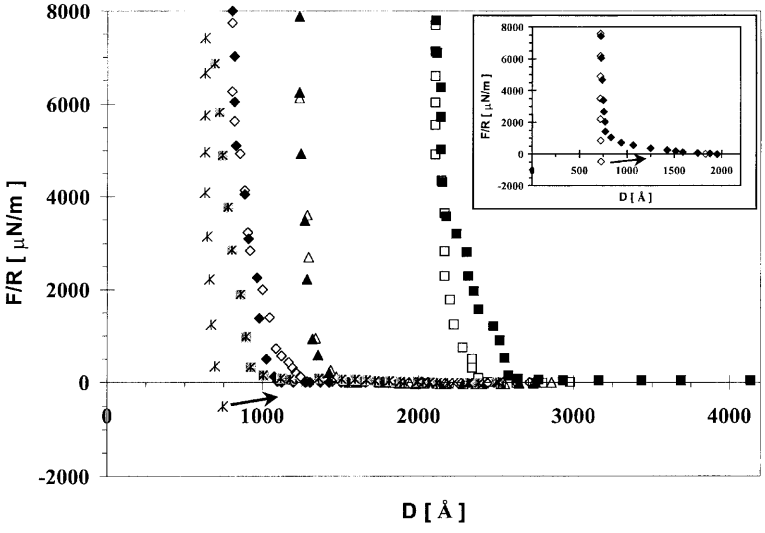

Fig. 5. Normal forces profiles measured for increasing humidity on approach (*filled symbols*) and separation (*open symbols*) of the HPC-covered surfaces RH: 0% (*squares*), 23% (*triangles*), 75% (*diamonds*), and 97% (*crossed squares, stars*) *Inset*: force profiles measured on approach and separation of the HPC-covered surfaces for RH = 75% in experiments with decreasing humidity. The *arrows* show the positions of abrupt jumps of the surfaces apart, for which a "pull-off" force was measured

RH = 0 on both approach and separation, in contrast to the results obtained for dry cellulose surfaces [15]. The profiles measured at 23% < RH < 75% showed no notable hysteresis upon approach and separation of the surfaces, i.e., the onsets of repulsion and the slopes of the forces profiles were very close. For RH = 75% a weak hysteresis was measured: the force profile measured on separation moved about 150 Å inwards. The major difference between the forces measured in the compression and the decompression cycles was observed for RH = 97%. While on approach the surfaces exhibited repulsion, upon separation an attraction force of about 560 μN/m was measured for $D = 740$ Å. The magnitude of attraction force increased to 1400 μN/m when the surfaces were maintained under compression to 600 Å for 20 min. Upon drying the layer, for RH = 0, 23, and 45% the force hysteresis measured in the compression–decompression cycles was similar to that in experiments performed for increasing humidity. The difference existed for RH = 75% only. While in experiments with increasing RH, the repulsion forces were measured both on approach and separation of the surfaces, in experiments with decreasing RH a noticeable attraction force of about 500 Å was measured when the surfaces receded (Fig. 5, inset).

Finally, since it was anticipated that following an increase in the RH, the binding energy of HPC to mica could be reduced, the variation in the lateral mobility of the layer and possible "pressing out" of the layer from the gap between the surfaces was examined by careful inspection of the appearance of the FECO patterns, as described by Lowack and Helm [16]. First, the variation in the shape of even interference fringes was monitored when the surfaces approached and separated at RH = 0. No change in the shape of the even fringes was observed following an increase in the normal force to up to

10,000 μN/m. When the RH was increased to 23% and the normal force reached about 1,000 μN/m, the tips of the even fringes became rippled. Upon surface retraction, the shape of the even fringes returned to its original state only after 6 ± 2 h. Following an increase in the RH to 75% and then to 97%, the shape of the even fringes did not change significantly: for a particular normal load (typically about 500–700 μN/m) some undulations appeared on the tip of the fringes; these distortions annealed 1–2 h after surface separation.

Discussion

Cellulose ethers have amphiphilic nature resulting from the presence in their molecules of hydrophilic glucose groups and hydrophobic alkyl chains; therefore, cellulose derivatives adsorb on both hydrophilic and hydrophobic surfaces [17]. Adsorption of HPC on mica most likely occurs via interactions of glucose units with the hydrophilic surface of mica. On the other hand, HPC is a typical associative polymer, often used as an associative thickener, and in semidilute solutions it forms supramolecular structures [18]. This feature explains the adsorption of scarce HPC clusters on the surface of mica following its short time exposure to the polymer solution, as is shown in Fig. 2a. A gradual temporal transformation of the clusters into fiberlike filaments and then into mature close-packed fibers is a characteristic hierarchy in self-assembly of macromolecules with limited flexibility [19]. A substantial compliance of the HPC layer is typical for the fiberlike layers formed by relatively low molecular weight polymers: a similar feature was earlier observed for short-chain "hairy-rod" polypeptide molecules adsorbed on mica [20]. Despite its reasonably small roughness, the HPC layer contained many voids and capillaries whose role in sorption of water will be discussed later.

In the surface force measurements, the distance between the surfaces corresponding to the onset of normal repulsion forces gives approximately the double thickness of the adsorbed layer; hence, the original thickness of the fiberlike layer of HPC on mica at RH = 0, $d_{HPC,RH=0,}$ was 1,375 ± 25 Å. This value was close to the thickness of a single layer of HPC fibers adsorbed on the mica substrate.

The variation in the thickness of the HPC layer following an increase in the amount of adsorbed water in the layer in experiments with increasing RH is shown in Fig. 6a. In this figure, the relative change in the thickness of the layer is expressed as $d_{HPC,RH}/d_{HPC,RH=0}$, where $d_{HPC,RH}$ is the layer thickness measured for a particular value of RH. The values of $d_{HPC,RH}$ and $d_{HPC,RH=0}$ were found from Fig. 3, whereas the concentration of water in the HPC layer for each value of the RH was obtained from Fig. 1, curve a.

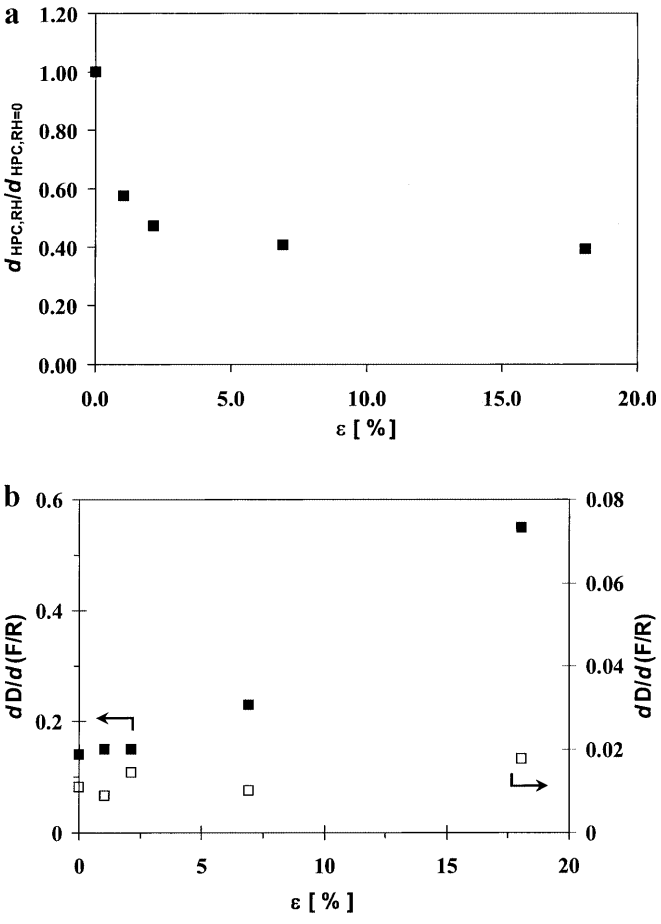

Fig. 6. Effect of the concentration of adsorbed water in the HPC layer on (**a**) the relative reduction in layer thickness and (**b**) the compressibility of the layer: soft part (*filled squares*) and "hard wall" (*open squares*). The variation in the thickness of the HPC layer is expressed as $d_{HPC,RH}/d_{HPC,RH=0}$, where $d_{HPC,RH}$ is the thickness of the layer for the particular value of RH and $d_{HPC,RH=0}$ is the thickness of the layer measured in dry air. The concentration of water in the layer for each value of the RH is extracted from Fig. 1, curve a

Several striking features follow from the comparison of Figs. 1 and 6a. First, when the humidity increased from 0 to 43%, the increase in the concentration of water in the layer was about 2%. Nevertheless, absorption of this relatively small amount of water by HPC caused a reduction in the layer thickness by a factor of 2.5. Second, a further increase in the RH to 75% and then to 97% led to a substantial increase in the water concentration in the HPC layer. Nevertheless, under these conditions the thickness of the layer decreased by less than 10% in comparison with the value measured for RH = 43%. Overall, following an increase in the RH in the SFA from 0 to 97% the thickness of the HPC layer shrank to about 40% of its original value.

The variation in the compressibility $dD/d(F/R)$ of the HPC layer following an increase in the amount of

moisture in the layer is shown in Fig. 6b. The compressibility for different values of the RH was extracted from the slopes of the logarithmic–linear graphs $F/R = f(D)$ in Fig. 3. When the amount of water in the HPC was below 3 wt%, the compliance of the layer did not change notably. A significant increase in compressibility occurred when the concentration of adsorbed water exceeded 8 wt% for RH = 75%, and especially for RH = 97%. In the latter case, the compliance of the layer was 3 times as great as for RH = 0%. In contrast, the compressibility of the rigid part of the HPC layer did not noticeably change with an increase in the RH, as can be seen from Fig. 6b. It should be noted that even for the thinnest and the most compliant HPC layer equilibrated under RH = 97%, the mica–mica contact was never reached, indicating that under compression the adsorbed layers remained in the gap between the surfaces. Moreover, to the best resolution we never observed black holes on the tips of even fringes, indicating the discontinuity of the refractive index of the HPC layer.

The change in the thickness of the adsorbed HPC layers in response to increasing RH could be caused by a combination of four effects: increase in the layer thickness owing to penetration of water to the HPC–mica interface and swelling of HPC, on one hand, and thinning of the layer owing to an increase in the lateral mobility of HPC molecules and partial polymer dissolution on the other hand.[2] While all four factors could partly contribute to the variation in layer properties, the net change in the layer thickness was dominated by the last two factors, which will be discussed later.

The increase in the lateral mobility of adsorbed molecules in response to increasing RH was thoroughly studied for monolayers of surfactants and polyelectrolytes [16, 21, 22]. In our work, the rippled shape of even fringes pointed to the change in the layer topography and to possible lateral transfer of HPC for $F/R > 500$–1,000 μN/m. However, for weaker forces no change in the FECO was noticed; thus it was assumed that the layer thickness measured at $F/R < 10$ μN/m was not affected by lateral expulsion of HPC from the gap between the surfaces. In contrast to thin confined films studied previously [16, 21, 22], annealing of the deformed HPC layers took a relatively long time after surface decompression, which could be caused by the fiberlike structure of adsorbed HPC.

In contrast to the change in layer thickness, weaker binding of HPC to the substrate at high RH could play an important role in studies of HPC compressibility. Indeed, with an increase in the RH, the compliance of the soft part of the layer increased significantly; however, this effect was not amplified for high normal loads, as it could be anticipated that substantial lateral transfer of HPC took place. On the contrary, for the high normal loads an increase in the RH did not play a crucial role in the layer compliance, as is shown in Fig. 6b, open symbols.

The variation in the properties of the adsorbed HPC layer in response to increasing humidity, as well as the change in the compressibility of the layer, can be best explained by the change in its supramolecular structure, as is illustrated schematically in Fig. 7. For simplicity, a single mica substrate is shown, covered with a monolayer of HPC fibers. In Fig. 7a a dry, fiberlike HPC layer is sketched, which has the largest thickness and the highest resistance to compression in comparison with the layers equilibrated at higher values of the RH. When the humidity in the chamber increased from 0 to 43%, adsorption of water on the fiberlike layer most likely occurred owing to capillary condensation in the voids between the HPC fibers, which resulted in the formation of numerous air–water menisci (Fig. 7b). In addition, molecular adsorption of water molecules occurred on –O–H and -C = O sorption sites in the glucose units on the surface of HPC fibers. Water is a relatively good solvent for HPC: the Flory–Huggins parameter is 0.43 [23]; thus, following the formation of water channels between the HPC fibers, the polymer began to dissolve, and the layer shrank, as shown in Fig. 7c. The reduction in the layer thickness occurred owing to a significant free volume in the layer localized in the capillaries and pores between the fibers, as well as inside the fibers, which had a network structure [24]. As the RH increased, water diffused

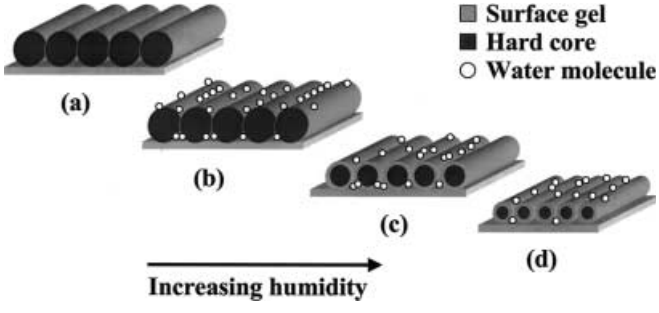

Fig. 7a–d. Transformation in the structure of the fiberlike HPC layer following adsorption of water. For simplicity, only a single layer of fibers is shown on the mica surface. **a** Dry HPC layer; **b** capillary condensation of water vapors in interstitial space between fibers; **c** dissolution of the outer part of the HPC fibers; **d** formation of surface gel

[2] Localization of water at the mica–HPC interface following an increase in the RH was observed in several AFM experiments. It should be admitted that mica is a very hydrophilic substrate and, hence, can play a crucial role in adsorption of water by the HPC layer. In fact, owing to this effect the concentration of moisture in the HPC layer adsorbed on mica can be higher than measured in the weighing experiments. Nevertheless, the position of the "rigid wall" measured under strong compression and especially the results obtained in shear studies of adsorbed HPC layers indicate that on the experimental time scale HPC–mica interactions are sufficiently strong and are not screened by the water located at the interface between the mica and the HPC.

toward the inner part of the fibers (Fig. 7d); however, the same slope of the hard-wall part of the force profiles measured for RH varying from 0 to 97% indicated that even for RH = 97%, water did not reach the inner part of the fibers. The variation in the properties of the adsorbed layer, such as its thickness, recovery upon drying, compliance, and hysteresis in compression–decompression cycles was governed by the change in the soft shell of the fibers which contained most of the adsorbed water. The structure of this shell, especially for $\epsilon = 18$ wt% (RH = 97%), could be best represented by that of the surface gel [7]. The process of gelation in the outer part of the adsorbed HPC layers at high values of RH explained the more gradual decrease in the layer thickness for RH > 45%, since water sorption led mostly to an increase in the concentration of moisture in the gel-like layer, and the substantial increase in the layer compliance shown in Fig. 6b. The appearance of attraction between the surfaces measured for RH = 97% and the dependence of the magnitude of the attraction force on the contact time indicated that time-dependent structural rearrangements and molecular interpenetration occurred in the compressed gel-like layer.

Similarly, weak hysteresis measured in compression–decompression cycles for RH < 45% indicated that fast relaxation of the HPC layer occurred after its compression, which resulted from the weak penetration of water inside the fibers. The structure of the HPC layer at RH = 75% is marginal. In experiments with increasing RH, an amount of water of about 7.3% caused weak hysteresis in the compression–decompression profiles; however, the forces acting between the surfaces on their approach and separation remained essentially repulsive (Fig. 5). In experiments with decreasing RH, the concentration of moisture in the layer was 10.0 wt%, i.e., somewhat higher owing to the slower desorption of the water immobilized in the gel-like layer. In addition, the distribution of water in the gel-like HPC layer equilibrated for a longer time under high ambient humidity could be more uniform. Both factors lead to attraction between the HPC layers upon their decompression (inset to Fig. 5).

A striking feature of the HPC layers is their "memory," i.e., the almost complete recovery of the layer thickness when the RH in the apparatus decreased from 97 to 0% (Fig. 3, filled symbols). This recovery, caused by evaporation of water from the soft shell of the fibers, was practically independent of the value of the RH.

In contrast, the recovery in the compressibility, characterized by the position of the hard wall in Fig. 4, depended on the value of the RH. For RH = 75%, the layer compliance did not change notably, whereas for RH = 0 and 23% (i.e., for essentially rigid fibers) the compressibility of the layer reduced significantly. Since the concentrations of water in the layer in experiments with increasing and decreasing RH were very close, the different compliance of the layer could be caused by the irreversible structural rearrangements in the gel-like shell of the fibers following their equilibration at different RH. These changes occurred owing to the interaction of water with HPC rather than as a result of the layer compression, since for low RH a very weak hysteresis was measured in approach–separation cycles.

Conclusion

We have characterized the variation in normal quasi-equilibrium interactions between adsorbed HPC layers as a function of ambient humidity. Our results reveal that the fiberlike HPC layers shrink following adsorption of moisture presumably owing to a significant free volume in the layer. The variations in the layer thickness, the compressibility, the compression–decompression hysteresis, and its recovery upon drying were explained by the existence of two types of structure in the HPC layers. For low RH, adsorption of moisture by the fiberlike layer occurs owing to capillary condensation. When the ambient humidity is high, water penetrates inside the HPC fibers, and the resulting structure is a rigid fiber core coexisting with the surface gel-like shell. The formation of the surface gel on the surface of the fibers following adsorption of moisture has important implications on fiber–fiber bonding (especially, time-dependent interactions) and their interactions with other materials, for example, inorganic particles [25].

Acknowledgements The authors acknowledge financial support of this work by the Pulp and Paper Consortium and NSERC Canada and fruitful discussions with D. Reeves, R. Pelton, and D. Gorin.

References

1. Karlson L, Joabsson F, Thuresson K (2000) Carbohydr Polym 41:25
2. Malmsten M, Tiberg F (1993) Langmuir 9:1098
3. Kusano H, Kimura S, Kitagawa M, Kobayashi H (1997) Thin Solid Films 295:53
4. Fukumori Y, Yamaoka Y, Ichikawa H, Fukuda T, Takeuchi Y, Osako Y (1988) Chem Pharm Bull 36:1491
5. Chan LW, Heng PWS, Wan LSC (1997) J Microencapsulation 14:545
6. Bottorff K (1994) Tappi J 77:105
7. Werbowyj RS, Gray DG (1980) Macromolecules 13:69
8. Berthold J, Olsson RJO (1998) Cellulose 5:281
9. Karlsson A, Singh SK (1998) Drug Dev Ind Pharm 24:827

10. Remunan-Lopes C, Bodmeir R (1996) Drug Dev Ind Pharm 22:1201
11. Israelachvili JN (1973) J Colloid Interface Sci 44:259
12. Seo M, Kumacheva E J Colloid Polym Sci (to be submitted)
13. Wrick MG, Waldam MH (1970) J Appl Polym Sci 14:579
14. Kumacheva E (1998) Prog Surf Sci 58:75
15. Holmberg M, Berg J, Stemme, S, Odberg, L, Rasmusson, J, Claesson P (1997) J Colloid Interface Sci 186:369
16. Lowack K, Helm CA (1995) Macromolecules 28:2912
17. Malmsten M, Lindman B (1993) Langmuir 9:1098
18. Freyssingeas E, Thuresson K, Nylander T, Joabson F, Lindman, B (1998) Langmuir 14:5877
19. Kitaev V, Schillen K, Kumacheva E (1998) J Polym Sci Part B Polym Phys 36:1567
20. Kitaev V, Kumacheva E (1998) Langmuir 14:5568
21. Chen YLE, Gee, ML, Helm CA, Israelachvili JN, McGuiggan PM (1989) J Phys Chem 93:7057
22. Chen U-L, Israelachvili JN (1992) J Phys Chem 96:7752
23. Barton AFM (1990) CRC handbook of polymer–liquid interaction parameters and solubility parameters. CRC, Boca Raton, p 219
24. Takahashi A, Shimazaki M, Yamamoto J (2001) J Polym Sci Part B Polym Phys 39:91
25. Pelton R (1993) Nord Pulp Pap Res J 1:113
26. Greenspan L (1997) J Res Natl Bur Stand USA 81A:89